A hydraulic and morphological criterion for upstream slopes in local-scour holes

Report W-DWW-93-255

G.J.C.M. Hoffmans
Road and Hydraulic Engineering Division
P.O. Box 5044
2600 GA Delft

july, 1993

CONTENTS

1 Introduction

Scour is a natural phenomenon caused by the flow of water in rivers and streams. Scour occurs naturally as part of the morphological changes of rivers and as result of structures man-made. Several types of scour can be distinghuished.
Experience has shown that due to sand or flow slides or micro instabilities at the end of the bed protection, the scour process can progressively damage the bed protection, leading eventually to the failure of the hydraulic structure for which the bed protection was meant. The length of the bed protection depends on the permissible amount of scour (maximum scour depth and the upstream scour slope) and the geotechnical structure of the soil involved (Pilarczyk, 1984).
In the scope of the Dutch Delta works, a systematical investigation of time scale for two and three-dimensional local scour in loose sediments was conducted by Delft Hydraulics and the Department of Public Works (Rijkswaterstaat). From model experiments on different scale and bed materials, relations were derived in order to predict the steepness of the upstream scour slope (De Graauw and Pilarczyk, 1981 and De Graauw, 1983).
Since the predictability of these relations is poor, especially for prototype conditions, a theoretical study concerning upstream scour slopes is carried out. In the present study a stability criterion is deduced which is based on the mass-balance equation and a stochastical bed-load predictor (Van Rijn, 1985) and fitted using approximately 250 clear-water scour experiments. In addition a empirical relation for undermining is discussed.
The stability criterion for upstream scour slopes and the model relation for undermining are verified applying some prototype experiments (Delft Hydraulics, 1979 and De Graauw & Pilarczyk, 1981).

2 Time phases of the scour process

2.1 *General*

To give some insight into the scour process behind hydraulic structures, the flow pattern and the sediment transport along the upstream slope of the scour hole are described for several phases in the scour process. Based on experiments at scale model with small Froude numbers (Breusers, 1966 and Dietz, 1969) Zanke (1978) distinguished four phases in the evolution of a scour hole: an initial phase, a development phase, a stabilization phase and an equilibrium phase.

2.2 *Initial phase*

In the initial phase the flow in the scour hole is nearly uniform in the longitudinal direction. This phase of the scour process can be characterized as the phase in which the erosion capacity is most severe compared to the erosion capacity in the remaining phases of the scour process.
Observations showed (e.g. Breusers, 1966) that at the beginning of the scour hole development a certain amount of bed material near the upstream scour slope goes into suspension. Most of these suspended particles are convected with the main flow and remain in suspension due to the internal balance between the upwards diffusive flux and the convective (downwards) flux, figure 1. Some of these particles will deposit and

will go into suspension again due to the large bursts of the turbulent flow near the bed, and some particles with a jump height smaller than a defined saltation or reference height are transported as bed load.

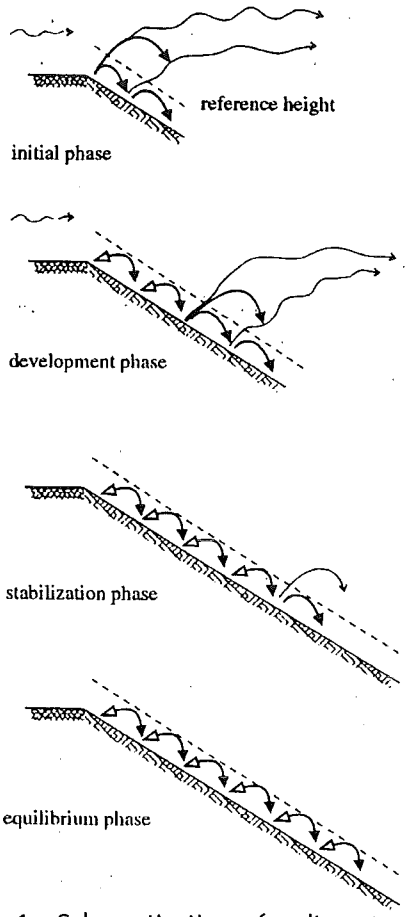

Figure 1 Schematization of sediment transport along upstream scour slope

2.3 *Development phase*

In the development phase the forms of the scour hole are similar. At this time the ratio of the maximum scour depth and the distance from the end of the bed to the point where the scour hole is at maximum is, more or less, constant.

After the transition of the bed protection to the erodible bed, the separated shear layer appears to be much like an ordinary plane mixing layer. The centre of the mixing layer is at the very beginning slightly curved caused by the influence of the bed. The curvature increases with the distance from the end of the bed protection, especially near the reattachment point. A recirculation zone develops with a flow direction opposite to the mean flow direction, figure 2.

Measurements of Hoffmans (1990) showed that the upper part of the upstream scour slope is in equilibrium, whereas the lower part is still in motion. In the recirculation zone the suspended load close to the bed is decreased significantly compared to the conditions in the initial phase. This can mainly be ascribed to the lowering of the bed flow velocities in time, despite the increase of the turbulence energy.

Though bed particles are picked up and convected by the flow, the time-averaged value of the sediment transport in the upper part of the upstream scour slope is negligibly small, since the contribution of the sediment transport due to the instantaneous flow velocities in the main direction equals approximately the transport due to the instantaneous flow velocities against the main direction.

2.4 *Stabilization phase*

In the stabilization phase the development of the maximum scour depth increases degressively. The erosion capacity in the deepest part of the scour hole is of no importance compared to the erosion capacity downstream from the point of reattachment, so that the dimensions of the scour hole increase more in the streamwise direction than in the vertical direction.

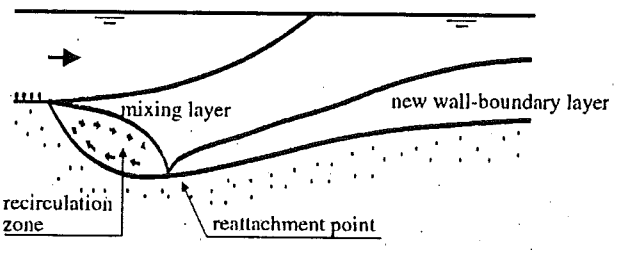

Figure 2 Flow regions

The more the scour process continues, the more the flow velocities above the lower part of the upstream scour slope decrease. In the stabilization phase the equilibrium situation for both the upstream scour slope and the maximum scour depth is almost achieved.

2.5 *Equilibrium phase*

The equilibrium phase can be defined as the phase in which the dimensions of the scour hole do no longer change significantly.
Generally in this phase of the scour process the bed particles at the upstream scour slope are only rolling and sliding beneath a saltation height.

3 Transport mechanism

3.1 *General*

The transport of sediment by a flow can be divided into two categories: the bed-load (transport) and the suspended-load (transport). Usually bed load is defined as the transport of particles of bed material which are sliding and rolling immediately above the bed. If under given flow conditions sediment particles are jumping above a defined saltation height, then these particles are assumed to be transported as suspended load.
The problem of defining critical flow conditions associated with initial instability and entrainment of bed sediment particles is of fundamental importance to predict the sediment transport mechanism.
The first known treatise on initial bed grain instability using the concepts of Prandtl and Von Kármán on boundary flow was produced by Shields (1936), who described the problem using the following basic parameters: the fluid density, the sediment density, the kinematic viscosity, the mean particle size and the bed shear-stress.
When the flow velocity over a bed of non-cohesive material has increased sufficiently, individual grains begin to move in an intermittent and random fashion. The initial bed instability results from the interaction between two statistically distributed random variables. At first every grain on the bed surface can be assumed to be potentially susceptible to an instantaneous critical bed shear-stress. The equilibrium of the grain becomes unstable if the instantaneous bed shear-stress exceeds the critical one. Due to the random shape, weight and placement of the individual grains, these critical shear stresses will have a probability distribution, which defines the initial movement characteristics of the bed material. The other random variables in the process of initial bed instability result from the variations in the action of the instantaneous bed shear-stresses generated by the flow. The probability that the instantaneous bed shear-stress is larger than a characteristic critical one is a measure for the transport of sediment.

3.2 *Bed boundary condition*

One of the most fundamental problems of sediment transport is the process that controls the exchange of sediment particles between the bed load and suspended load layer (boundary condition). A particle leaving the bed starts its trajectory by following a saltation. A particle can enter the suspension layer when it is lifted to a level at which the upward turbulence-induced forces are comparable to or higher than the submerged particle weight.
Although in a flow with solid transport no sharp distinction can be made for bed load

and suspended load, a suspension layer and a bed layer can be defined for reasons of simplicity. In the upper layer sediment particles are conveyed in suspension due to the turbulent eddy-diffusivity, which is prevailing over the vertical motion. In the bed layer the bed load depends on the local composition of the sediment and the local characteristics of the flow.

3.3 *Mass-balance equation*

The continuity equation per unit width for the total sediment transport s (i.e. the sum of bed load and suspended load) in the scour hole can be expressed as:

$$\frac{\partial z_b}{\partial t} + \frac{\partial s}{\partial x} = 0 \qquad (1)$$

in which z_b is the bed level, t is time and x is the longitudinal coordinate.
In the equilibrium phase of the scour process when the bed in the recirculation zone is in equilibrium, i.e., when the erosion capacity is nil, the sediment transport equals approximately the upstream sediment supply.

3.4 *Bed load*

Several expressions, more or less empirical, have been suggested during the last century to compute bed load as a function of flow characteristics and particle diameter. Here a bed load formula introduced by Van Rijn (1985) and modified by Hoffmans (1992) is used to predict upstream scour slopes in the equilibrium phase of the scour process.
According to Van Rijn (1984), bed load is computed as the product of the saltation height, the particle velocity and the bed-load concentration. The equations of motion for a solitary particle, as given by White and Schulz (1977), are solved numerically to determine the saltation height and particle velocity. Simple relations for the saltation height are proposed and calibrated by both a mathematical model and a large number of flume experiments.
In the equilibrium phase of the scour process the (time-averaged) bed load at the upstream scour slope is negligibly small, since the bed shear-stress is marginal in comparison with the critical one. However, due to sweeps and ejections (Lu and Willmarth, 1973), which occur during burst, bed particles are lifted up. Due to the acceleration of gravity the bed particles are deposited, so these particles are hopping randomly at the upstream scour slope without moving significantly with the main flow.

3.5 *Shear stresses*

The standard deviation σ_0 of the instantaneous bed shear-stress τ_0 determines, together with the effective (mean) bed shear-stress $\mu\bar{\tau}_0$, the bed load to a large extent. In addition, the sediment transport is also influenced by the sediment characteristics such as the density of the material, the sediment-size distribution, the shape of the particle and the porosity of the (non-cohesive) material.

Bed shear-stress

Generally the (mean) bed shear-stress $\bar{\tau}_0$ or the bed shear-velocity u_* decreases enormously from the, more or less, uniform flow at the fixed bed to the erodible bed (figure 3). Downstream from the separation point the absolute value of the bed shear-

stress at the upstream slope is relatively small compared to the bed shear-stress in the new wall-boundary layer. In the recirculation zone the bed shear-stress is directed against the main flow, and in the new wall-boundary layer downstream from the point of reattachment the bed shear-stress increases gradually.

Characteristic critical bed shear-stresses
Applying a classical approach of sediment mechanics, i.e. the sediment particles are only moving and rolling along the bed surface (no suspension), the following relations can be given for a sediment particle resting on a two-dimensional slope, figure 4 (downslope):

$$\hat{\tau}_1 = \hat{\tau}_c \frac{\sin(\phi - \theta)}{\sin\phi} \qquad (2)$$

and (upslope):

$$\hat{\tau}_2 = -\hat{\tau}_c \frac{\sin(\phi + \theta)}{\sin\phi} \qquad (3)$$

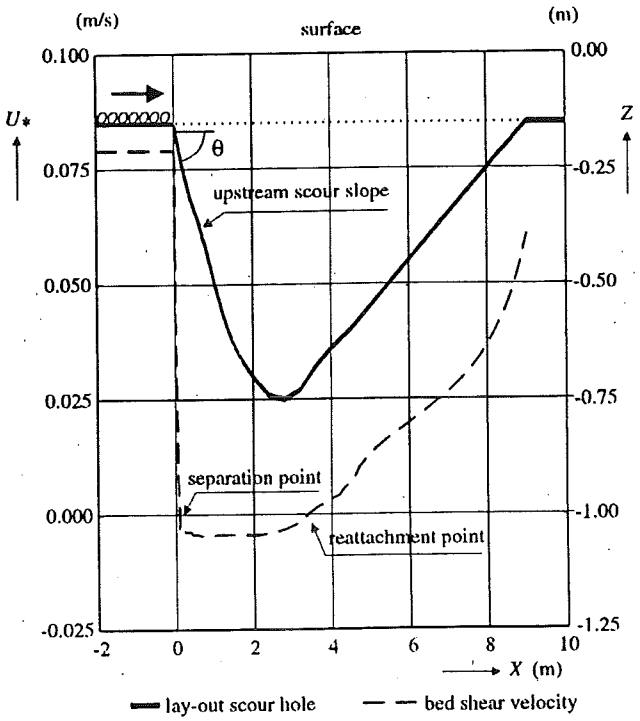

(Meijer et al., 1992)

Figure 3 Bed shear-velocity as a function of the longitudinal distance

in which $\hat{\tau}_1$ and $\hat{\tau}_2$ are characteristic critical bed shear-stresses, $\hat{\tau}_c$ ($\simeq 1.5\bar{\tau}_c$) is the characteristic critical bed shear-stress for uniform flow, $\bar{\tau}_c$ ($= \rho u_{*,c}^2$) is the (mean) critical bed shear-stress according to Shields, ρ is the fluid density, $u_{*,c}$ is the critical bed shear-velocity, ϕ is the angle of repose and θ is the slope angle, i.e. the angle between the upstream scour slope and the horizontal.

Instantaneous bed shear-stress
The influence of turbulence on bed load has been investigated by several researchers in the past. As given by Kalinske (1947) and Einstein (1950) the instantaneous flow velocity varies according to a Gaussian distribution. The idea of Kalinske was picked up by Van Rijn (1986) who postulated an instantaneous transport parameter, which is an expression for the fluctuating mobility of the particles in terms of the stage of the fluctuating movement relative to the critical stage for initiation of motion.
For reasons of simplicity Van Rijn assumed that the instantaneous bed shear-stress τ_0 is normally distributed. However, this distribution can be questioned, since measurements of Lu and Willmarth (1973) show that the influence of sweeps and ejections, whose contribution is larger than the contribution of the inward and outward interaction, is not included in the Gaussian distribution. The phenomena sweeps, which are directed to the bed, and ejections, which are moving away from the bed, contribute most to the turbulent shear stresses. More details concerning sweeps and ejections can be found in Lu and Willmarth (1973) and Hoffmans (1992).

4 Upstream scour slopes

4.1 *General*

The upstream slope in a local-scour hole is defined here as the slope between the coordinates $x = h_0/30$ and $x = h_0/2$. Generally this slope reaches an equilibrium and is less steep than the tangent at the transition from the fixed to the erodible bed.
Based on theoretical grounds a hydraulic and morphological stability criterion is derived for predicting the steepness of upstream scour slopes. In addition a simple criterion for undermining is found. These criteria are calibrated using a large number of flume experiments, in which the material properties and the hydraulic and geometrical conditions were varied.

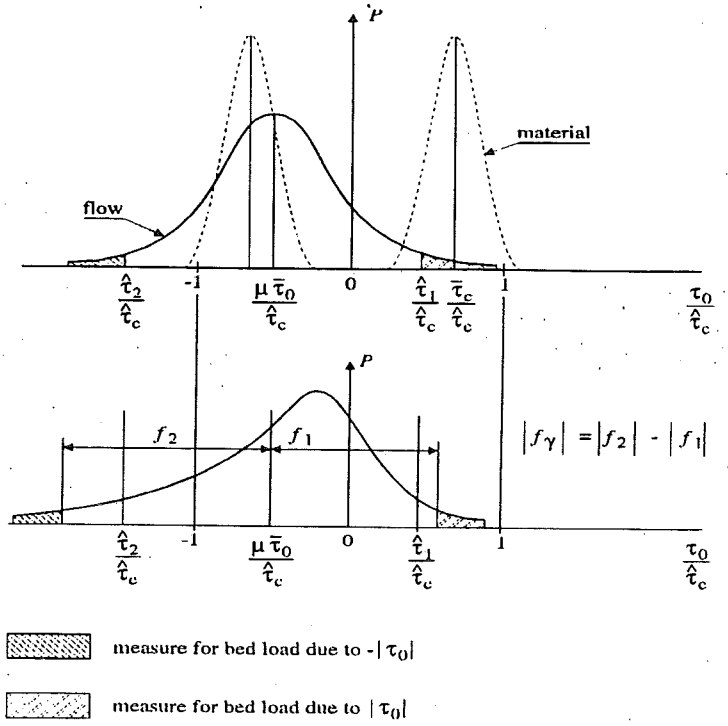

Figure 4 Schematization of probability distribution of flow and material characteristics in non-uniform flow

4.2 *Earlier investigations*

Based on a thorough investigation of scour downstream from an apron Dietz, (1969, 1973) reported that the upstream scour slope depends on a turbulence level, the form of the flow velocity profile and a dimensionless parameter given by:

$$\delta = \frac{(\bar{U}_0 - \bar{U}_c)D_*}{w} \tag{4}$$

which is related to the flow and sediment characteristics, $\bar{U}_0$ (initial depth-averaged flow velocity), $\bar{U}_c$ (critical depth-averaged flow velocity), w (fall velocity of the bed material) and D_* (sedimentological diameter).
For nearly identical hydraulic structures, Dietz found a relation between the slope angle and δ . However, this relation is not unambiguous, when the relative turbulence intensity is not constant but varies due to different geometrical conditions.
As given by Breusers et al. (1977) many parameters can be distinguished which may influence the scouring phenomenon. Somewhat arbitrary, Kolkman (1980) and Buchko (1986) combined some of these parameters, resulting in:

$$\operatorname{cotan}\theta = f\left[\frac{d_{50}\sqrt{\Delta g d_{50}}}{\nu},\ \Delta,\ \frac{d_{50}}{h_0},\ \frac{\bar{U}_0}{\sqrt{\Delta g d_{50}}}\right] \tag{5}$$

in which d_{50} is the mean bed particle, Δ is the relative density, g is the accel-

eration of gravity, v is the kinematic viscosity and h_0 is the initial flow depth. The idea of this concept was that each parameter could be varied independently from the other ones. Kolkman argued that for fine sand the influence of the kinematic viscosity (term 1) could also be expressed differently by introducing the fall velocity, so that:

$$\operatorname{cotan}\theta = f\left[\frac{w}{\sqrt{\Delta g d_{50}}},\ \Delta,\ \frac{d_{50}}{h_0},\ \frac{\bar{U}_0}{\sqrt{\Delta g d_{50}}}\right] \tag{6}$$

Though the dimensionless parameters are important, the theoretical consideration can be questioned, since the influence of turbulence in the recirculation zone is not taken into account.
Based on the research activities of Dietz, Kolkman and the socalled 'systematical scour research' data (Delft Hydraulics, 1972, 1979), the slope angle was represented by (De Graauw and Pilarczyk, 1981):

$$\operatorname{cotan}\theta = 5.5\frac{w}{d_{50}}\left[\frac{v}{\Delta^2 g^2}\right]^{1/3}\left[2.5 + \frac{0.75}{\alpha - 1.32}\right] \tag{7}$$

The value of the turbulence coefficient α can be obtained from previous model investigations or from scale models for complex hydraulic constructions.
Several expressions for α have been deduced from the tests in the systematical series. These relations, which include the influence of the roughness of the bed protection and the effects of both two and three-dimensional flow, are summarized in a scour manual (Van der Wal et al., 1991).
Later, after evaluating the enormous amount of data of the scour experiments, De Graauw (1983) found that the upstream scour slope is a function of the turbulence coefficient only:

$$\operatorname{cotan}\theta = 2.3 + \frac{1}{\alpha - 1.3} \tag{8}$$

4.3 *Hydraulic and morphological stability criterion*
The stability of the upstream scour slope is the result of the interaction between fluid motion and material properties. The equilibrium situation of upstream scour slopes for non-cohesive material is achieved here by equalization of bed load due to the instantaneous bed shear-stresses sloping downward and bed load due to the instantaneous bed shear-stresses sloping upward.
Assuming a Gaussian (symmetrical) distribution for τ_0, and if only clear-water scour is considered, thus no upstream sediment transport is present, the following relation can be derived (appendix A):

$$\frac{\hat{\tau}_1 + \hat{\tau}_2 - 2\mu\bar{\tau}_0}{\hat{\tau}_c} = 0 \tag{9}$$

where μ is an efficiency factor where the influence of the bed roughness is taken

into account (appendix B). Generally the bed of the upstream scour slope is hydraulically smooth for which applies $\mu \simeq 1$.
In order to include the influence of sweeps and ejections it seems reasonable to assume that the probability distribution of τ_0 has long tails for extreme values for τ_0 . The skewness of the probability distribution for τ_0 could be expressed by (figure 4):

$$\frac{\hat{\tau}_1 + \hat{\tau}_2 - 2\mu\bar{\tau}_0}{\hat{\tau}_c} + f_\gamma = 0 \qquad (10)$$

Consequently the slope angle can be written as (appendix B):

$$\theta = \arcsin\left(f_\tau + \tfrac{1}{2}f_\gamma\right) \quad \text{with} \quad f_\tau = -\frac{\mu\bar{\tau}_0}{\hat{\tau}_c} \simeq 2.9 * 10^{-4}\frac{\bar{U}_0^2}{\Delta g d_{50}} \qquad (11)$$

in which f_γ is a measure for the skewness.
Though the effective bed shear-stress $\mu\bar{\tau}_0$ determines the slope angle, its influence on the steepness of the upstream scour slope compared to the influence of sweeps and ejections (modelled by f_γ) is relatively small, especially for experiments at scale model with small Reynolds numbers (appendix B).
When θ exceeds a critical value, i.e. for $\arcsin(f_\tau + \tfrac{1}{2}f_\gamma) > \phi'$ with ϕ' is the angle of internal friction, micro instabilities could occur, undermining the end of the bed protection. Sand and flow slides of the soil under the bed protection may even be possible, however, these phenomena are strongly dependent on the soil properties, e.g. the contraction and the elastic compressibility of loose sand (De Groot et al., 1992).
Since little information was available regarding the material properties of the scour experiments (e.g. the porosity, the angle of repose, angle of internal friction were not measured), the aforementioned criterion is not extensively examined.
A simple criterion for gradual undermining is discussed in section 4.4 which is, more or less, based on trial and error.

Closure problem
To optimize the function f_γ in equation 10, the hydraulic parameters have to be known.
Since the instantaneous bed shear-stress is not unambiguously defined (Hoffmans, 1992), it is assumed for reasons of simplicity that the parameter f_γ is closely related to the relative turbulence intensity r_0 just upstream from the scour hole and the effective bed roughness k_s of the bed protection.
The material properties are characterised here by the mean bed particle d_{50} , the particle

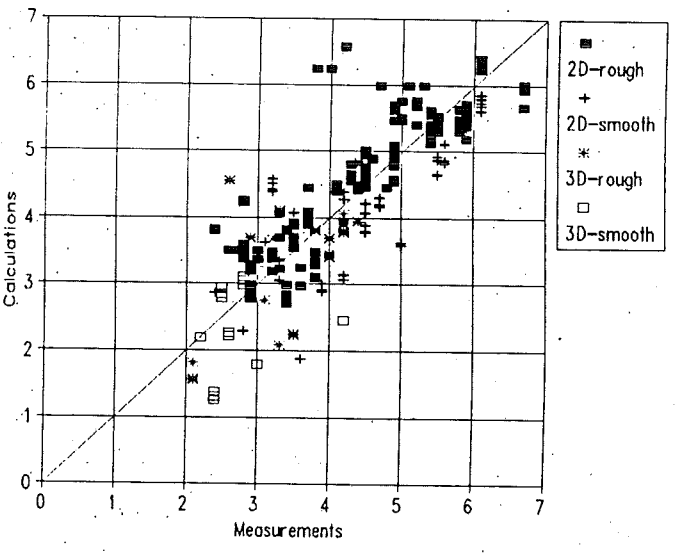

Figure 5 Calculated and measured cotan θ

diameter d_{90} (for which 90% of the mixture is smaller than d_{90}) and the relative density, so the influence of the distribution of the mixture and the density of the bed material (polystyrene, bakelite, sand) is taken into account.
More than 250 experiments (Delft Hydraulics, 1972 , 1979 and Buchko, 1986) were used to find the best compromise between the measured and calculated angle of the slope, resulting in (figure 5):

$$f_\gamma = (0.22 + 1.5r_{0,m})f_C \quad \text{with} \quad f_C = \frac{\delta_0^*}{\delta^*} \simeq \frac{C}{C_0} \tag{12}$$

in which $r_{0,m}$ is the measured relative turbulence intensity, δ^* is the displacement thickness, C is the Chézy coefficient and $C_0 = 40 m^{1/2}/s$. For hydraulically-rough conditions, i.e. for $C \leq 40 m^{1/2}/s$ regarding the fixed bed before the scour hole, the roughness function measures $f_C = 1$.
In these laboratory experiments not only the hydraulic conditions (discharge Q and initial flow depth h_0) were varied but also the geometrical conditions (length of the bed protection L , height of the sill D and the bed roughness). Moreover, tests were executed with an abutment in permanent flow introducing three-dimensional scour.
To determine the predictability of the aforementioned relations for upstream scour slopes, the discrepancy ratio r (i.e. the ratio between the measured and calculated upstream scour slope) is computed using experiments of Delft Hydraulics (1972, 1979) and Buchko (1986). The measured upstream scour slopes were obtained directly from the measurements, whereas the calculated ones (equations 7 and 8) were determined using a 'measured' turbulence coefficient (e.g. Hoffmans, 1993).
This analysis, in which a distinction has been made between two and three-dimensional flow (table 1), shows that compared to the other empirical relations, upstream scour slopes can be calculated more accurately with the model relation given in this study.

references	$0.90 < r < 1.11$		$0.80 < r < 1.25$		$0.67 < r < 1.50$	
	2D n = 201	3D n = 65	2D (201)	3D (65)	2D (201)	3D (65)
De Graauw and Pilarczyk (1981)	15%	6%	34%	51%	58%	65%
De Graauw (1983)	50%	25%	85%	40%	97%	78%
Hoffmans (1993)	59%	37%	85%	71%	95%	78%

Table 1 Comparison of computed and measured upstream scour slope

4.4 *Undermining*
The phenomenon of undermining can be defined as the erosion which occurs at the end of the bed protection. In addition to the gradual undermining due to the composition of the bed, a sudden undermining may occur (sand or normal slide), when the slope angle of the bed is larger than the angle of internal friction.
According to Delft Hydraulics (1979) and Blazejewski (1991), the dangerous undermining of the vertical edge of the bed protection results from the higher turbulence energy

and the larger erosion capacity of the flow in the recirculation zone due to the higher turbulence energy directly upstream from the scour hole. Measurements at scale model with sand as scour material (Delft Hydraulics, 1979 and Buchko, 1986) have shown that the end of the bed protection is undermined if a dimensionless parameter α_u defined as:

$$\alpha_u = \frac{\alpha \bar{U}_{0,m} - \bar{U}_c}{\bar{U}_0} \quad \text{with} \quad \alpha = 1.5 + 4.4 r_0 f_c \tag{13}$$

exceeds a critical value $\alpha_{u,c} \simeq 1.75$. For two-dimensional scour, the maximum depth-averaged flow velocity $\bar{U}_{0,m}$ equals about $\bar{U}_0$, whereas for three-dimensional scour $\bar{U}_{0,m}$ depends strongly on the geometry upstream from the scour hole, for example by an obstacle or an abutment in the flow.

In this study the characteristic undermining $z_u(t_1)$ is defined as the undermining which would occur when the maximum scour depth equals approximately the initial flow depth. The dimensionless undermining $z_u(t_1)/h_0$ as a function of α_u is shown in figure 6. Though a distinction has been made between flexible and fixed beds, the type of bed protection seems to be of secondary importance compared to α_u.

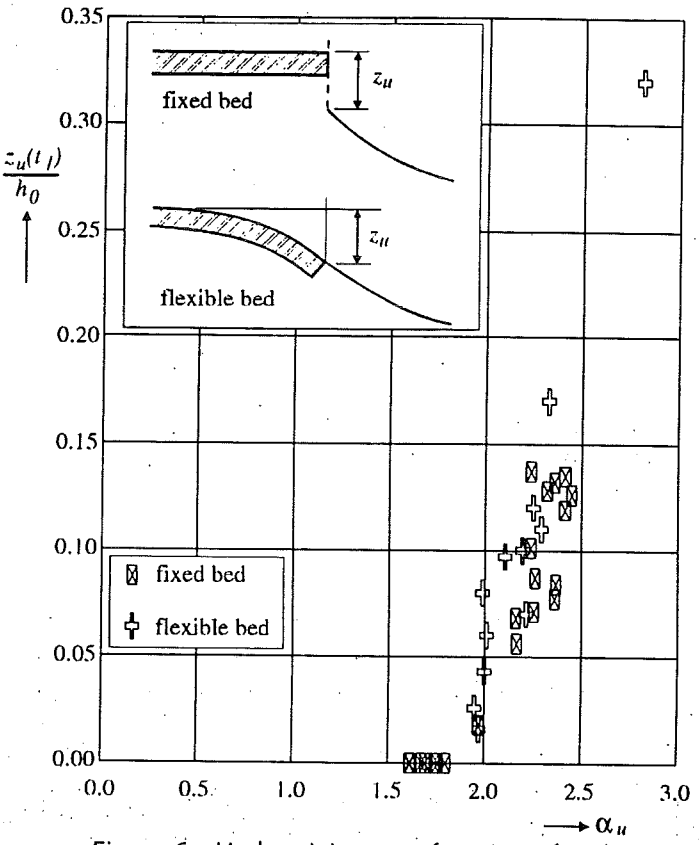

Figure 6 Undermining as a function of α_u

5 Verification with prototype data

5.1 *General*

Within the scope of research activities with respect to scour behind the storm surge barrier and compartment dams in the Eastern Scheldt, some experiments on prototype scale were carried out (De Graauw and Pilarczyk, 1981). For this purpose the sluice in the Brouwersdam was chosen which was built to refresh the brackish water in the Grevelingen lake for environmental reasons. The experiments were executed to study the influence of clay layers to scour and to verify scour relations obtained from scale models.

5.2 *Hydraulic conditions*

The discharges and flow velocities regarding the two experiments were almost similar,

whereas the soil characteristics were different.
The discharges, the flow levels and the bed configuration were measured frequently. Also some flow velocity and concentration measurements in the centre of the sluice were carried out. During the experiment the sea water was discharged into the lake during the flood and out during the ebb. The last had no influence on the development of the scour hole, because of the relatively small flow velocities above the scour hole during the ebb. The suspended load from the sea into the lake was also negligible.
The sluice consisted of a sill 5.4 m height with two side constrictions equal to 2.5 m on the left side and 1.5 m on the right side. The flow depth was about 10 m and the length of the bed protection from the toe of the sill measured about 50 m. The effective roughness of the bed protection is estimated to be 0.4 m. The other dimensions of the sluice are presented in figure 7.
The soil characteristics with respect to experiment A were measured beforehand. The diameter of the bed material varied with the depth from 0.2 to 0.3 mm. Some thin clay lenses on different levels were present, especially in the upper soil-layer between 2

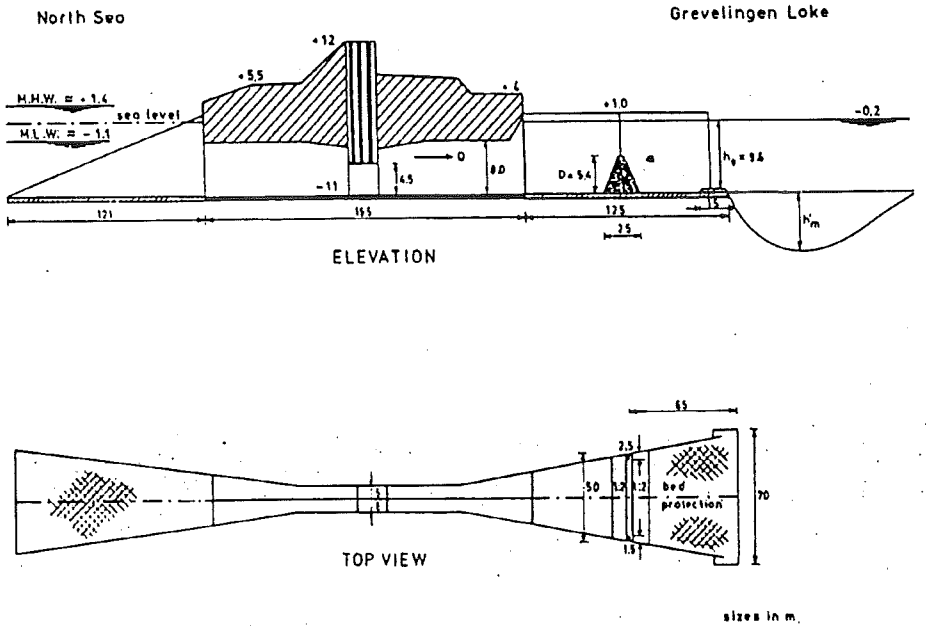

Figure 7 Prototype situation (Brouwersdam)

and 4 meters below the original bed. The thickest clay layer of about 0.2 m was situated at about 3.5 m below the bed. The other clay lenses were mostly in the range of 0.01 to 0.02 m of about 0.2 m.
The developed scour hole was refilled with loosely-packed material. The bed material regarding experiment B consisted of fine sand with a mean particle diameter of about 0.260 mm. The particle diameter for which 90% of the mixture is smaller than d_{90} measured 0.29 mm.
As a result of ebb and flood not only the flow velocity varies in time but also the sediment transport. To simulate the scour process a characteristic depth-averaged flow

velocity is introduced which is defined as the depth-averaged flow velocity, which would occur if the sediment transport does not vary in time.

5.3 *Discussion*

Figure 8 shows some measured bed profiles of the considered prototype experiments at different moments, whereas the gradual undermining, including a sand slide, is shown in figure 9. The calculations of both the upstream scour slopes ($\text{cotan}\theta \simeq 2.$) and the undermining ($z_u/h_0 \simeq 0.25$) agree with the measurements reasonably. The computations are obtained with equations 11 and 13. More details of experimental and computational results can be found in appendix D.

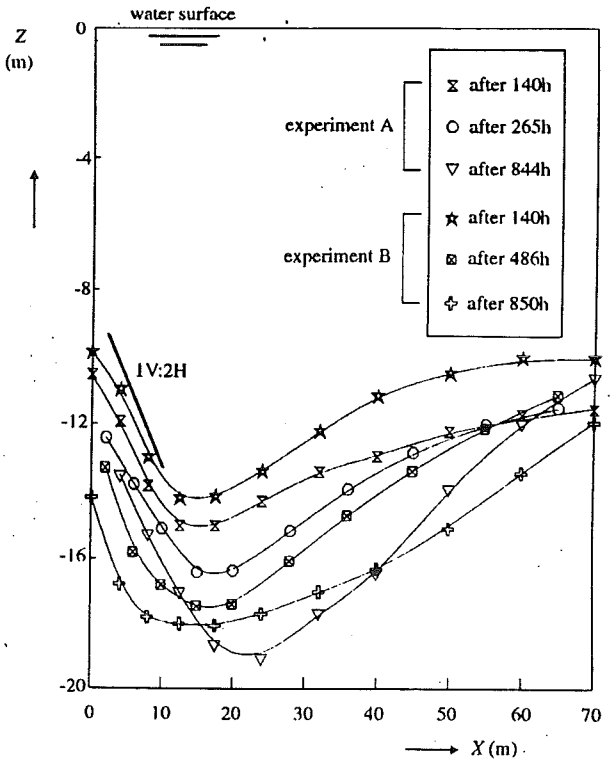

Figure 8 Bed profiles of scour holes (Brouwersdam)

Due to the tidal influence the flow velocities vary in time. In experiment A and B the maximum flow velocities averaged over about 140 tides measured by approximation 1.2 m/s (Hoffmans, 1992). With this assumption and using the stability criterion (equation 11) it follows that $\text{cotan}\theta \simeq 1.8$. Generally the angle of internal friction for sand lies in the range of 30 to 40 degrees and depends on the porosity, the particle diameter and the distribution of the mixture.

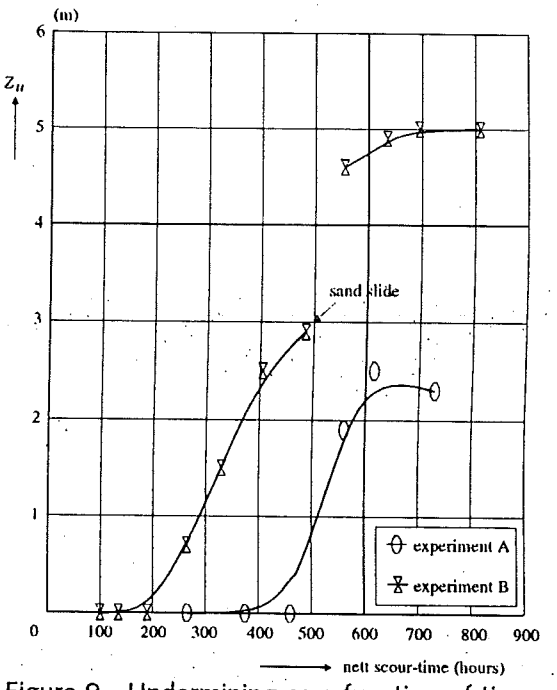

Figure 9 Undermining as a function of time

Micro instabilities can be predicted when the flow velocities are larger than 1.3 m/s ($\phi' = 30°$) or 1.9 m/s for $\phi' = 40°$. During the experiments flow velocities were measured varying from 1.5 to 2.0 m/s. Since micro instabilities and a sand slide after approximately 450 hours (nett-scour time) were observed, the stability criterion seems to be feasible for practical engineering. When the sub-soil consists of clay and sand layers the results obtained from equation 11 must be interpreted carefully, because the influence of the cohesion of the sub-soil is not taken into account.

6 Conclusions

A hydraulic and morphological stability criterion for upstream scour slopes has been derived which is calibrated using a large number of flume experiments and verified for two prototype experiments. Despite the simplifications made in the closure problem, this study shows a way to calculate the steepness of upstream slopes in the equilibrium phase of the scour process for non-cohesive material. Moreover, the criterion is able to predict micro instabilities.

Appendix A Stability criterion

A hydraulic and morphological stability criterion for upstream scour slopes in the equilibrium phase of the scour process is derived applying a stochastical bed-load predictor (Van Rijn, 1986). The stability criterion regards clear-water scour only. The equilibrium situation of upstream scour slopes for non-cohesive material is achieved by equalization of bed load due to the instantaneous bed shear-stresses τ_0 sloping downward and bed load due to τ_0 sloping upward. Thus the time-averaged bed load along the slope is assumed to be nil.
As given by Van Rijn (1986), bed load can be related to a stochastical entrainment parameter E_m for both uniform and non-uniform flow. The contribution of E_m caused by τ_0 sloping downward reads:

$$E_{m,1}(\gamma) = \int_0^{\infty} (T_m(\tau_0))^{\gamma} P(\tau_0)\, d\tau_0 \qquad (A_1)$$

and the contribution due to τ_0 against the main flow direction is:

$$E_{m,2}(\gamma) = \int_{-\infty}^{0} (T_m(\tau_0))^{\gamma} P(\tau_0)\, d\tau_0 \qquad (A_2)$$

In equations A_1 and A_2, T_m expresses the mobility of bed particles as a function of τ_0, P is the probability distribution of τ_0 and γ ($\simeq 2.0$) is a constant. Assuming P to be Gaussian distributed, a further elaboration of equations (A_1) and (A_2) yields (Hoffmans, 1992):

$$E_{m,1}(\gamma) = \frac{1}{\sqrt{2\pi}} \left[\frac{\sigma_0}{\hat{\tau}_c}\right]^{\gamma} \int_0^{\infty} \xi^{\gamma} e^{-\frac{1}{2}(\xi - \xi_1)^2}\, d\xi \qquad (A_3)$$

$$E_{m,2}(\gamma) = \frac{1}{\sqrt{2\pi}} \left[\frac{\sigma_0}{\hat{\tau}_c}\right]^{\gamma} \int_0^{\infty} \xi^{\gamma} e^{-\frac{1}{2}(\xi - \xi_2)^2}\, d\xi \qquad (A_4)$$

where $\xi_1 = (\mu\bar{\tau}_0 - \hat{\tau}_1)/\sigma_0$ and $\xi_2 = (-\mu\bar{\tau}_0 + \hat{\tau}_2)/\sigma_0$ are dimensionless parameters, μ is an efficiency factor (appendix B), $\hat{\tau}_1$, $\hat{\tau}_2$ and $\hat{\tau}_c$ are characteristic critical bed shear-stresses (section 3) and σ_0 is the standard deviation of the instantaneous bed shear-stress.
With the assumption that $E_{m,1} \simeq E_{m,2}$, the following stability criterion for upstream scour slopes in the equilibrium phase of the scour process is obtained:

$$\xi_1 = \xi_2 \rightarrow \hat{\tau}_1 + \hat{\tau}_2 - 2\mu\bar{\tau}_0 = 0 \qquad (A_5)$$

Appendix B Effective bed shear-stress

In appendix B a discussion is given concerning the influence of the effective bed shear-stress $\mu\bar{\tau}_0$ on upstream scour-slopes in the equilibrium phase of the scour process. The influence of $\mu\bar{\tau}_0$ is compared to the influence of sweeps and ejections.
Assuming a Gaussian distribution for the instantaneous bed shear-stress τ_0 the following relation can be deduced (appendix A):

$$\frac{\hat{\tau}_1 + \hat{\tau}_2 - 2\mu\bar{\tau}_0}{\hat{\tau}_c} = 0 \qquad (B_1)$$

in which $\hat{\tau}_1$, $\hat{\tau}_2$ and $\hat{\tau}_c$ $(= \hat{\alpha}_c\bar{\tau}_c)$ are characteristic critical bed shear-stresses (section 3.5), $\bar{\tau}_c$ is the critical bed shear-stress and $\hat{\alpha}_c \simeq 1.5$ is a constant (De Ruiter, 1982, 1983). The efficiency factor μ reflects the roughness of the bed and can be approximated by (Hoffmans, 1992):

$$\mu = \left(\frac{\ln \frac{12h}{k_s}}{\ln \frac{12h}{k_s'}} \right)^2 \qquad (B_2)$$

in which h is the flow depth, k_s is the effective bed roughness, which is by approximation equal to the mean dune height, $k_s' \simeq 3d_{90}$ and d_{90} is the particle diameter for which 90% of the mixture is smaller than d_{90} .
The influence of the phenomena sweeps and ejections in the probability distribution for τ_0 could be described by:

$$\frac{\hat{\tau}_1 + \hat{\tau}_2 - 2\mu\bar{\tau}_0}{\hat{\tau}_c} + f_\gamma = 0 \qquad (B_3)$$

in which f_γ is a measure for the skewness of the probability distribution.
Expressing $\hat{\tau}_1$ and $\hat{\tau}_2$ in terms of θ (slope angle) and ϕ (angle of repose) yields:

$$\frac{\sin(\phi - \theta)}{\sin\phi} - \frac{\sin(\phi + \theta)}{\sin\phi} - \frac{2\mu\bar{\tau}_0}{\hat{\tau}_c} + f_\gamma =$$

$$= -\frac{2\sin\theta\cos\phi}{\sin\phi} - \frac{2\mu\bar{\tau}_0}{\hat{\tau}_c} + f_\gamma = 0 \qquad (B_4)$$

Hence θ can be given by:

$$\theta = \arcsin\left(c_\phi\left(f_\tau + \tfrac{1}{2}f_\gamma\right)\right) \quad \text{with} \quad f_\tau = -\frac{\mu}{\hat{\alpha}_c}\frac{\bar{\tau}_0}{\bar{\tau}_c} \qquad (B_5)$$

in which $c_\phi = \tan\phi$ and for a primary estimation ϕ is assumed to be 45°, so that

$c_\phi \simeq 1.0$. Based on the results of various investigators, there seems to be dependency of the ϕ-value on the slope angle. Lysne (1969) reported a value of $\phi \simeq 38°$ for a bed sloping upward and a value of $\phi \simeq 50°$ for a bed sloping downward. Fernandez-Luque and Van Beek (1976) found a value of $\phi \simeq 47°$ for a bed sloping downward.
To proceed with examining the influence of the effective bed shear-stress on upstream scour slopes some definitions are given. The friction coefficient C_f and the critical bed shear-stress $\bar{\tau}_c$ are defined as:

$$C_f = \frac{\bar{\tau}_0}{\frac{1}{2}\rho \bar{U}_m^2} \qquad (B_6)$$

$$\bar{\tau}_c = \rho \Psi_c \Delta g d_{50} \qquad (B_7)$$

in which ρ is the fluid density, $\bar{U}_m$ is the time-averaged flow velocity in the outer flow (of course, $\bar{U}_m = \bar{U}_0$ and $\bar{U}_0$ is the initial depth-averaged flow velocity) Ψ_c is the critical mobility-parameter, Δ is the relative density, g is the acceleration of gravity and d_{50} is the mean particle diameter.
In the equilibrium phase of the scour proces $\bar{\tau}_0$ is directed against the main flow, thus $f_\tau > 0$. Combining equations B_5, B_6 and B_7 gives:

$$f_\tau = \frac{\frac{1}{2}\mu C_f}{\hat{a}_c \Psi_c} \frac{\bar{U}_0^2}{\Delta g d_{50}} \qquad (B_8)$$

Computations with both the flow models DUCT and ODYSSEE have shown that in the equilibrium phase of the scour proces the bed shear-stress at upstream scour slopes is, more or less, constant. For nearly in equilibrium scour holes the friction coefficient measures approximately $5.5 * 10^{-5}$ (Meijer et al., 1992). However, for scour holes where the expansion ratio h_m/h_0 (ratio between the maximum flow depth and the initial flow depth) is about 1.5 the friction coefficient is significantly larger than $5.5 * 10^{-5}$. Predictions of the flow model DUCT as well as laser Doppler measurements show that C_f is related to the geometry of the scour hole, table B1.
Vanoni et al. (1967) have noted that the critical mobility-parameter for the fully-rough turbulent zone, i.e. for $\Psi_c = 0.06$, corresponds to a low but measurable bed load. At

h_m/h_0	k_s (mm)	slope	$\bar{U}_0$ (m/s)	$C_{f,m}$ (*10^{-5})	C_f (*10^{-5})	reference
5	0.5	1V:2.5H	0.77		5.5	Meijer et al., 1992
5	0.5	1V:2.5H	1.16		5.5	
2	6.0	1V:2H	0.40	31	10	Hoffmans,1988
3	6.0	1V:4H	0.41	7.5	3.1	
1.4	2.5	1V:2H	0.52	59	36	Van Mierlo and De
1.3	2.5	1V:2H	0.63	73	32	Ruiter, 1988

Table B1 Friction coeffient C_f

values of 0.03 and even less, occasional movement of single grains may occur.
Assuming that the bed of the upstream scour slope is hydraulically smooth ($\mu \simeq 1$) the parameter f_τ due to the bed shear-stress is ($C_f = 5.5 * 10^{-5}$, $\Psi_c = 0.045$) :

$$f_\tau = \frac{c_\tau \bar{U}_0^2}{\Delta g d_{50}} \qquad (B_9)$$

in which c_τ ($\simeq 2.9 * 10^{-4}$) is a constant.
More than 300 experiments were used to calibrate f_γ resulting in (section 4.3):

$$f_\gamma \simeq 0.22 + 1.5 r_0 \qquad (B_{10})$$

in which r_0 is the relative turbulence intensity at the transition of the fixed to the erodible bed.
Consequently the ratio between f_τ and f_γ measures:

$$\frac{f_\tau}{f_\gamma} \simeq \frac{2.9 * 10^{-4}}{0.22 + 1.5 r_0} \frac{\bar{U}_0^2}{\Delta g d_{50}} \qquad (B_{11})$$

Generally the turbulence upstream from the scour hole is dying out to uniform flow conditions, provided the length of the bed protection is sufficient large, that is approximately 80 to 100 times the initial flow depth.
Figure B1 shows combinations of $\bar{U}_0$ and d_{50} for which applies $f_\tau/f_\gamma = 0.1$. The computational results are obtained using sand as bed material $\Delta = 1.65$. In addition the relative turbulence intensity at the transition of the fixed to the erodible bed is assumed to be $r_0 = 0.15$. For experiments at scale model ($\bar{U}_0 < 1$m/s) the influence of the bed shear-stress is of no importance compared to the influence of the large instantaneous bed shear-stresses. However, for prototype conditions (Brouwersdam) where the sub-soil consists of fine sand and where flow velocities larger than 1 m/s occur, prudence has to be called. Then the influence of the bed shear-stress can not simply be neglected.

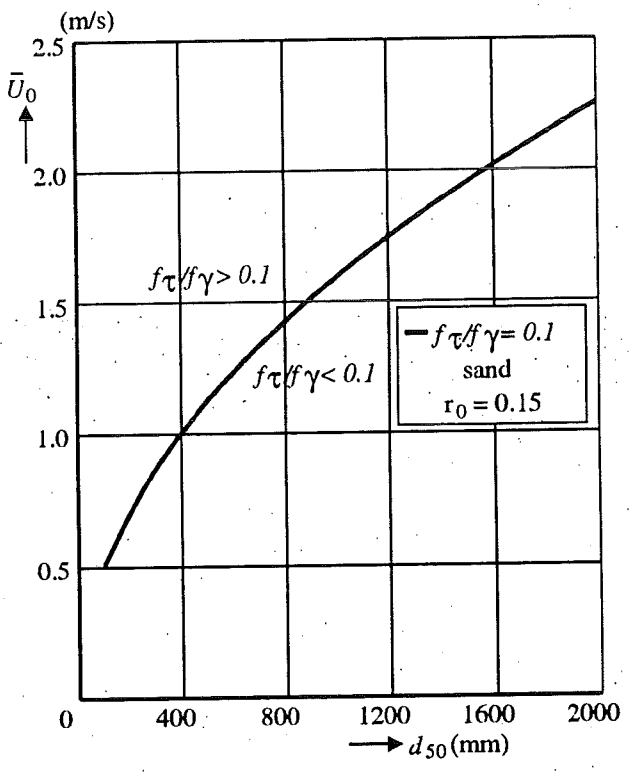

Figure B1 Combinations of $\bar{U}_0$ and d_{50} for $f_\tau/f_\gamma = 0.1$

Appendix C **Undermining parameters**

Tables C1 and C2 provide an overview of the most relevant parameters which can undermine hydraulic constructions. More details concerning the hydraulic conditions of the experiments such as the flow velocities, the length of the bed protection, the roughness of the bed etc. can be found in Delft Hydraulics (1979) and Buchko (1986). The turbulence coefficient α, the relative turbulence intensity r_0 and the dimensionless parameter α_u are computed according to formulae given in section 4. The relative undermining $z_u(t_1)/h_0$ is obtained by interpolation of two profile measurements of the PROVO. In the last column of both tables the condition of the bed protection just upstream from the scour hole is given.

series	α	r_0	α_u	$z_u(t_1)/h_0$	condition
t01	1.93	0.09	1.70	0	fixed
t02	1.93	0.09	1.74	0	fixed
t03	1.93	0.09	1.62	0	fixed
t04	1.93	0.09	1.68	0	fixed
t05	1.93	0.09	1.76	0	fixed
t06	1.93	0.09	1.80	0	fixed
t07	2.49	0.22	2.24	0.101	fixed
t08	2.49	0.22	2.32	0.128	fixed
t09	2.61	0.25	2.36	0.132	fixed
t10	2.70	0.27	2.45	0.126	fixed
t11	2.49	0.22	2.24	0.137	fixed
t12	2.57	0.22	2.26	0.087	fixed
t13	2.57	0.22	2.41	0.119	fixed
t14	2.57	0.22	2.41	0.135	fixed
t15	2.57	0.22	2.37	0.084	fixed
t16	2.57	0.22	2.16	0.056	fixed
t17	2.57	0.22	2.36	0.077	fixed
t18	2.57	0.22	2.16	0.068	fixed
t19	1.93	0.09	1.61	0	fixed

Table C1 Computational and experimental results (Buchko, 1986)

series	α	r_0	α_u	$z_u(t_1)/h_0$	condition
1t0.1	2.50	0.23	2.25	0.071	fixed
1t2	2.50	0.23	2.21	0.070	flexible
1t1	2.50	0.23	2.25	0.120	flexible
1t3	2.50	0.23	2.29	0.110	flexible
1t11	2.50	0.23	2.33	0.170	flexible
2t0.2	2.21	0.16	1.97	0.018	fixed
2t4	2.21	0.16	1.97	0.016	flexible
2t7	2.21	0.16	2.01	0.060	flexible
3t5	2.32	0.19	1.99	0.080	flexible
3t6	2.32	0.19	2.10	0.097	flexible
4t8	2.50	0.23	2.20	0.100	flexible
4t9	2.50	0.23	2.81	0.320	flexible
5t12	2.21	0.16	1.95	0.026	flexible
5t13	2.21	0.16	2.00	0.043	flexible

Table C2 Computational and experimental results (Delft Hydraulics, 1979)

Appendix D **Results of prototype experiments Brouwersdam**

Both experimental and computational results of some prototype experiments near the Brouwersdam are given (tables D1 and D2). More details regarding the computation of the characteristic discharge, the critical depth-averaged velocity and the relative turbulence intensity (table D2) can be found in Hoffmans (1992, 1993).

experimental parameters	experiment A	experiment B
initial flow depth (scour hole) (m)	10.6	9.6
height sill (m)	5.4	5.4
length of the bed protection (m)	50	52
effective roughness of bed protection (m)	0.4	0.4
averaged discharge (m^3/s)	271	270
maximum discharge (m^3/s)	380	380
particle diameter (mm)	d_{50} = 0.25 d_{90} = 0.29	d_{50} = 0.26 d_{90} = 0.29
upstream scour slope at end of test	1V:2.2H	1V:1.1H
undermining just before sand slide (m)		2.9
undermining at end of test (m)	2.3	5.0
condition sub-soil	clay/sand	sand

Table D1 Experimental results

computational parameters	experiment A	experiment B
characteristic discharge (m^2/s)	9.89	9.89
characteristic depth-averaged velocity (m/s)	0.93	1.03
critical depth-averaged velocity (m/s)	0.41	0.41
relative turbulence intensity (-)	0.28	0.29
turbulence coefficient (-)	2.91	2.92
roughness function (-)	1.13	1.12
parameter α_u	2.47	2.52
parameter f_τ	0.09	0.10
parameter f_γ	1.03	1.04
upstream scour slope	1V:2.1H	1V:2.1H
undermining at $t = t_1$ (m)	2.0±1.0	1.8±1.0

Table D2 Computational results

References

Breusers, H.N.C., 1966, Conformity and time scale in two-dimensional local scour, Proceedings Symposium on model and prototype conformity, Hydraulic Research Laboratory, Poona, p.1-8.

Breusers, H.N.C., G. Nicollet and H.W. Shen, 1977, Local scour around cylindrical piers, Journal of Hydraulic Research, IAHR, Vol.15 No.3.

Blazejewski R, 1991, Prediction of local scour in cohesionless soil downstream of outlet works, Doctoral thesis, Agriculture University Poznan, Poland.

Buchko, M.F., 1986, Investigation of local scour in cohesionless sediments by using a tunnel model, Report No.Q239, Delft Hydraulics, Delft.

Delft Hydraulics, 1972, Systematical investigation of two and three-dimensional local scour, Investigation M648/M863/M847 (in dutch), Delft Hydraulics, Delft.

Delft Hydraulics, 1979, Prototype scour hole 'Brouwersdam', Investigation M1533 Part I,II,III and IV (in dutch), Delft Hydraulics, Delft.

Dietz, J.W., 1969, Kolkbildung in feinen oder leichten Sohlmaterialien bei strömendem Abfluß, Mitteilungen Heft 155, Universität Fridericiana Karlsruhe.

Dietz, J.W., 1973, Sicherung der Flußsohle unterhalb von Wehren und Sperrwerken, Wasserwirtschaft 63, No.3.

Einstein, H.A., 1950, The bed load function for sediment transportation in open channel flows, Technical Bulletin, No.1026, US Department of Agriculture, Washington D.C..

Fernandez-Luque, R. and R. van Beek, 1976, Erosion and transport of bed load sediment, Journal of Hydraulic Research, IAHR, Vol.14, No.2.

De Graauw, A.F.F., and K.W. Pilarczyk, 1981, Model-prototype conformity of local scour in non-cohesive sediments beneath overflow-dam, 19th IAHR-congress, New Delhi (**also** Delft Hydraulics, Publication No.242).

De Graauw, A.F.F., 1983, A review of research on scour, Report S562 (in dutch), Delft Hydraulics, Delft.

De Groot, M., Den Adel, H., T.P. Stoutjesdijk and K.J. van Westenbrugge, 1992, Risk analysis of flow slides, 23rd International Conference on Coastal Engineering, Venice.

Hoffmans, G.J.C.M., 1988, Flow model with prescribed eddy viscosity, Report No.11-88, Faculty of Civil Engineering, Hydraulic and Geotechnical Engineering Division, Delft University of Technology, Delft.

Hoffmans, G.J.C.M., 1990, Concentration and flow velocity measurements in a local scour hole, Report No.4-90, Faculty of Civil Engineering, Hydraulic and Geotechnical Engineering Division, Delft University of Technology, Delft.

Hoffmans, G.J.C.M., 1992, Two-dimensional mathematical modelling of local-scour holes, Doctoral thesis, Faculty of Civil Engineering, Hydraulic and Geotechnical Engineering Division, Delft University of Technology, Delft.

Hoffmans, G.J.C.M., 1993, A study concerning the influence of the relative turbulence intensity on local-scour holes, Report W-DWW-93-251, Ministry of Transport, Public Works and Watermanagement, Road and Hydraulic Engineering Division, Delft.

Kolkman, P.A., 1980, Parameters which may influence the scour process, unpublished notes, Delft Hydraulics, Delft.

Kalinske, A.A., 1947, Movement of sediment as bed load in rivers, Transactions, American Geophysical Union, Vol.28, No.4.

Lysne, D.K., 1969, Movement of sand in tunnels, Journal of Hydraulic Division, No.HY6, ASCE.

Lu, S.S. and W.W. Willmarth, 1973, Measurements of the structure of the Reynolds stress in a turbulent boundary layer, Journal of Fluid Mechanics, Vol.60, Part 3, p.481-511.

Meijer, D.G., Hoffmans, G.J.C.M. and A.K. Otta, 1992, Eddy viscosity modelling in nearly equilibrium scour holes, Delft Hydraulics, Delft.

Van Mierlo, M.C.L.M. and J.C.C. De Ruiter, 1988, Turbulence measurements above dunes, Report Q789, Vol.1 and 2, Delft Hydraulics, Delft.

Pilarczyk, K.W., 1984, Interaction water motion and closing elements, The Closure of Tidal Basins, p.387-405, Delft University Press, Delft.

Van Rijn, L.C., 1984, Sediment Transport, Part I: Bed load transport, Journal of Hydraulic Engineering, Vol.110, No.10, ASCE

Van Rijn, L.C., 1985, Mathematical models for sediment concentration profiles in steady flow, Euromech 192, Munich/Neubiberg, Germany, (**also** Delft Hydraulics, Publication No.365).

Van Rijn, L.C., 1986, Mathematical modelling of suspended sediment in non-uniform flows, Journal of Hydraulic Engineering, Vol.112, No.6, ASCE, (**also** Delft Hydraulics, Communication No.365).

De Ruiter, J.C.C., 1982, The mechanism of sediment transport on bed forms, Euromech 156, Mechanics of Sediment Transport, p.137-142, Istanbul.

De Ruiter, J.C.C., 1983, Incipient motion and pick-up of sediment as function of local variables, unpublished notes, Delft Hydraulics, Delft.

Shields, A., 1936, Anwendung der Ähnlichkeitsmechanik und der Turbulenzforschung auf die Geschiebebewegung, Mitteilungen Preussischen Versuchsanstalt für Wasserbau and Schiffbau, Nr.26, Berlin.

Vanoni, V.A. et al., 1967, Closure to discussion on "Sediment transportation mechanics: Initiation of motion", Journal of Hydraulic Division, ASCE.

White, B.R. and J.C. Schulz, 1977, Magnus effect in saltation, Journal of Fluid Mechanics, Vol.81, Part 3, p.497-512.

Wal, M. van der, G. van Driel and H.J. Verheij, 1991, Scour manual, Report Q647, Delft Hydraulics, Delft.

Zanke, U., 1978, Zusammenhänge zwischen Strömung und Sedimenttransport Teil 2: Berechnung des Sedimenttransportes hinter befestigten Sohlenstrecken, Sonderfall zweidimensionaler Kolk, Mitteilungen des Franzius-Instituts der TU Hannover, Heft 48,

List of symbols

c_1	coefficient	[-]
C	Chézy coefficient	$[L^{½}T^{-1}]$
C_f	friction coefficient	[-]
d	particle diameter	[L]
D	height of sill	[L]
D_*	sedimentological diameter; $d_{50}(\Delta g/\nu^2)^{1/3}$	[-]
E_m	stochastical entrainment parameter	[-]
f_c	roughness function	[-]
f_s	skewness parameter	[-]
f_τ	dimensionless bed shear-stress; $-\mu\bar{\tau}_0/\hat{\tau}_c$	[-]
g	acceleration of gravity	$[LT^{-2}]$
h	flow depth	[L]
h_0	initial flow depth	[L]
k_s	effective or equivalent bed roughness	[L]
k_s'	effective bed roughness related to the grains	[L]
L	length of bed protection	[L]
n	number (of experiments)	[-]
P	probability distribution	[-]
Q	discharge	$[L^3T^{-1}]$
r	discrepancy factor	[-]
r_0	relative turbulence intensity	[-]
s	sediment transport per unit width	$[L^2T^{-1}]$
t	time	[T]
t_1	characteristic time at which the maximum scour depth equals h_0	[T]
T_m	instantaneous transport parameter	[-]
u_*	bed shear-velocity	$[LT^{-1}]$
$u_{*,c}$	critical bed shear-velocity (Shields)	$[LT^{-1}]$
$\bar{U}_0$	initial depth-averaged flow velocity	$[LT^{-1}]$
$\bar{U}_c$	critical depth-averaged flow velocity	$[LT^{-1}]$
w	fall velocity	$[LT^{-1}]$
x	longitudinal coordinate	[L]
z	vertical coordinate	[L]
z_u	undermining at end of bed protection	[L]
α	turbulence coefficient; $1.5 + 4.4 r_0 f_c$	[-]
$\hat{\alpha}_c$	coefficient	[-]
α_u	dimensionless parameter; $(\alpha\bar{U}_{0,m} - \bar{U}_c)/\bar{U}_0$	[-]
γ	coefficient	[-]
δ	dimensionless parameter; $(\bar{U}_0 - \bar{U}_c)D_*/w$	[-]
δ^*	displacement thickness	[-]
Δ	relative density; $(\rho_s - \rho)/\rho$	[-]
θ	slope angle	[-]
μ	efficiency factor	[-]
ν	kinematic viscosity	$[L^2T^{-1}]$
ξ_1	dimensionless parameter	[-]
ρ	fluid density	$[M^3L^{-1}]$

List of symbols (continued)

ρ_s	material density		$[M^3L^{-1}]$
σ_0	standard deviation of τ_0		$[ML^{-1}T^{-2}]$
τ_0	instantaneous bed shear-stress		$[ML^{-1}T^{-2}]$
$\overline{\tau}_c$	critical bed shear-stress (Shields)		$[ML^{-1}T^{-2}]$
$\hat{\tau}_c$	characteristic critical bed shear-stress;	$\hat{\alpha}_c\overline{\tau}_c$	$[ML^{-1}T^{-2}]$
$\hat{\tau}_1$	characteristic critical bed shear-stress;	$\hat{\tau}_c\sin(\phi - \theta)/\sin\phi$	$[ML^{-1}T^{-2}]$
$\hat{\tau}_2$	characteristic critical bed shear-stress;	$-\hat{\tau}_c\sin(\phi + \theta)/\sin\phi$	$[ML^{-1}T^{-2}]$
$\overline{\tau}_0$	bed shear-stress		$[ML^{-1}T^{-2}]$
ϕ	angle of repose		[-]
ϕ'	angle of internal friction		[-]
Ψ_c	critical mobility-parameter		[-]

Subscripts

b	bed
c	critical
m	maximum or measured
0	initial or reference